



Durability studies of unsupported Pt cathodic catalyst with working time of direct methanol fuel cells

Zhen-Bo Wang^{a,*}, Yu-Yan Shao^a, Peng-Jian Zuo^a, Xin-Peng Wang^b, Ge-Ping Yin^a

^a Department of Applied Chemistry, Harbin Institute of Technology, Harbin 150001, China

^b Department of Physics, University of Puerto Rico, Rio Piedras Campus, San Juan, PR 00931, USA

ARTICLE INFO

Article history:

Received 17 June 2008

Received in revised form 30 July 2008

Accepted 20 August 2008

Available online 27 August 2008

Keywords:

Direct methanol fuel cell

Life test

Cathodic catalyst degradation

Electrochemically active surface area

In situ cyclic voltammetry

ABSTRACT

Life tests of direct methanol fuel cells (DMFCs) were carried out with three individual single cells for three different times. X-ray diffraction (XRD) and X-ray photoelectron spectra (XPS) were used to evaluate the cathodic Pt black catalysts prior to and after the life tests. XRD results showed that the particle sizes of cathodic catalysts increased from an original value of 7.3–8.3, 8.7, and 9.2 nm, whereas their lattice parameters first increased and then decreased from an original value of 3.9188–3.9210, 3.9197, and 3.9196 Å before and after 117, 210, and 312 working hours, respectively. XPS results indicated that the metal content gradually decreased with test time, but the contents of Pt oxides in cathodic catalysts increased. Hydrogen adsorption–desorption cyclic voltammetry were employed to test the performances of three individual fuel cells and the electrochemically active surface areas (S_{EAS}) of cathodic catalysts before and after the life tests. It is found that both S_{EAS} of cathodic catalysts and their utilization decreased markedly. This indicates that the change of S_{EAS} and utilization of cathodic catalysts are the main factors affecting the performance decay of DMFC. The dissolution/agglomeration of Pt metal from cathodic catalysts also plays an important role in the performance decay of DMFC. The sintering/degradations of cathodic Pt nanoparticles were accelerated due to crossover of methanol to form the mixed potentials. The agglomeration of cathodic Pt nanoparticles may be illustrated with dissolution/deposition mechanism.

© 2008 Elsevier B.V. All rights reserved.

1. Introduction

Low-temperature fuel cells with either hydrogen or methanol as the fuel represent an environmentally friendly technology, which are attracting much attention as portable energy system. Proton exchange membrane fuel cells (PEMFC) are moving steadily towards commercialization for various applications [1,2]. In recent years, direct methanol fuel cell (DMFC) has been receiving much more attention due to its advantages of easy transportation and storage of the fuel, a substantial reduction of system weight, size, and complexity without the need for reformers and humidifiers, and high-energy conversion efficiency [3]. The performance of DMFC depends on several factors, among which the most important are: (i) electrocatalytic activity and durability of catalysts, for example, the overpotential of anode, when operated with pure hydrogen, has a value of tens of microvolts. However, the overpotential caused by slower kinetics of oxygen reduction reaction at the cathode is more than 300 mV, even if pure Pt is used [4,5]; (ii) the ionic conductivity and resistance to methanol crossover of

proton exchange membrane (PEM); (iii) water and heat management on the cathodic side of the cell [6]; (iv) the aging of PEM. Researchers have made great efforts on the above factors [7–9], and obtained many good results. The performance of DMFC was enhanced markedly in recent years, but its price is still prohibitive, because a large amount of noble metals of Pt and Ru as the catalysts in anodes and cathodes are still used. In fact, the limitation of platinum resource and rareness of ruthenium have been the major obstacles to the broader commercialization of DMFCs. Hence, it is very worth prolonging the life of catalysts for DMFC and lowering their loading and the costs of DMFC by using various techniques. The performance degradation rates of DMFC are evidently higher than that of pure hydrogen PEMFC [10]. The commercialization of DMFC demands a stable operation for at least thousands of hours, e.g. 5000–40000 h required for fuel cell vehicles and residential power generators [11]. Many factors will affect the stable operation of DMFC, including the growth of catalytic particles, the loss of catalytic active components, poisoning of electrocatalysts by accumulated intermediates from methanol electrooxidation or impurities, aging of PEM, and changes of hydrophobic/hydrophilic properties in the catalyst layers and diffusion layers [12]. Thereinto, the electrocatalysts are one of the major components of membrane electrode assemblies (MEAs), and their stability plays an impor-

* Corresponding author. Tel.: +86 451 86417853; fax: +86 451 86413707.
E-mail address: wangzhenbo1008@yahoo.com.cn (Z.-B. Wang).

tant role in the long-term operation of fuel cells [13]. The catalyst degradation in DMFC proceeds gradually, and its degree is time-dependant. Wilson et al. [14] studied the particle growth of Pt catalyst after 4000 h of a continuous operation of fuel cells, and found that approximately 60% of the active surface area was lost. In addition, the characterization changes of catalysts at the anode and cathode in DMFC are different. Cathodes in DMFC operate in a serious corrosive environment, e.g. high water content, low pH value, high temperature, and high potentials gone with operating substantial oxygen partial pressures [15], and the carbon support may also be oxidized during fuel starvation [10]. So, the agglomeration and dissolution of catalyst in cathodes are more severe than that in anodes. But, a research showed that the catalyst agglomeration in anode is more serious than that in cathode, because methanol might be more aggressive against the catalyst than water produced in DMFC [16]. The durability investigations of cathodic and anodic catalysts were already carried out in details in a single DMFC in our previous work [17]. The contribution of cathodic catalyst to the performance degradation of DMFC is greater than that of anodic one. Two mechanisms for particle size growth, i.e. Ostwald ripening, and coalescence have been suggested [18–22]. Although coalescence has been reported to be insignificant for carbon supported catalysts at temperatures below 500 °C [19], this may not be the case with DMFC, in which metal black catalysts are typically used. The primary growth mechanism, Ostwald ripening, would be expected to be more serious at the cathode [22]. However, the aging mechanism of cathodic catalysts is not very clear at present. The debate about this question is still open. The changing regularity of cathodic catalysts with times in different individual single DMFCs is unexplored yet.

In our recently work, the change rules of anodic PtRu black catalysts with different working times in three individual single cells were investigated in detail [23]. In this paper, we focus on exploring the durability of cathodic catalysts for 117, 210, and 312 h, respectively, in three single DMFCs operated at 60 °C and a current density of 100 mA cm⁻². Electrochemical characterizations were performed prior to and after the life tests, and their results were compared. Results of XRD and XPS obtained before and after the life tests were also discussed.

2. Experimental

2.1. MEA preparation

The MEA preparation was prepared according to the method mentioned in the literatures [17,23]. As described briefly, Pt black and PtRu black (Johnson Matthey Co.) were used as catalysts for the cathode and anode, respectively. PtRu black and 5 wt.% Nafion[®] ionomer solution (DuPont EW = 1100) were mixed in isopropanol alcohol solution to form a homogeneous suspension for the anode. The cathodic catalyst ink was prepared similarly with Pt black, Nafion[®] solution, and PTFE latex. The Nafion[®] contents in both anodic and cathodic catalyst layers were 20 wt.%. The catalyst inks were deposited onto the gas diffusion layer (GDL) by paint brush with a metal loading of 4 mg cm⁻² for both electrodes. The carbon cloth (E-TEK, ELAT/NC/DS/V2 double sided ELAT electrode, carbon only, no metal, 20% wet proofed) was used as the GDL and backing layer for the cathode. The anodic GDL was prepared by using spray painting method with 1 mg cm⁻² of carbon black and 5% Nafion[®] ionomer solution on the carbon paper. DuPont Nafion[®] 117 membrane was used as solid electrolyte. Before being applied to the electrodes, the membrane was pretreated by dilute nitric acid (the ratio of nitric acid:deionized water of 18 MΩ cm by volume is 1:1) at its boiling temperature for 20 min, and then rinsed five times with ultrapure water. The membrane was then immersed in the

boiling ultrapure water for 1 h. The membrane electrode assembly (MEA) was formed by hot-pressing the anodic and cathodic diffusion layers onto the Nafion[®] film.

2.2. Electrochemical measurements

2.2.1. Single fuel cell tests

Single fuel cell tests were performed by using a homemade 5 cm² apparent area test fixture. The fixture was composed of a pair of graphite plates with serpentine flow fields for reactants to flow. Air and methanol solution were used as the reactants. The flow rate of air is 100 mL min⁻¹ under ambient pressure, and that of the solution is 2.5 mL min⁻¹ with a concentration of 1.0 mol L⁻¹ methanol. Both reactants were not humidified, and directly enter the cell. The cell temperature was 60 °C. Rod-like heaters were inserted into the plates to control the cell temperature. Polarization curves, power density curves, and potential–time curves were obtained by using a Fuel Cell Test Station (Scribner Associates Inc., Series 890B, Southern Pines, NC, USA) in a galvanostatic polarization mode. Potential–time curves of the three individual single cells were measured in a galvanostatic mode with a current density of 100 mA cm⁻² for 117, 210, and 312 h, respectively. To ensure that the electrolyte in Nafion[®] membrane and electrode is moist enough to have high ionic conductivity, it is necessary to activate the MEA before the performance measurements. In our experiments, the single cells were conditioned with ultrapure water and air at 60 °C for 5 h. After conditioning, ultrapure water was replaced with methanol solution of 1.0 mol L⁻¹ for 24 h in a galvanostatic mode with a current density of 10 mA cm⁻² prior to the acquisition of life test data.

2.2.2. Cyclic voltammetry (CV)

Cyclic voltammograms were obtained by using a PAR potentiostat/galvanostat (EG&G Model 273A) at a cell temperature of 25 °C. Fig. 1 shows a scheme of the experimental set-up for fuel cell testing and *in situ* cyclic voltammetric measurements [17,23]. Electrochemically active surface areas (*S*_{EAS}) of cathodic catalysts were determined by hydrogen adsorption–desorption test. For this, the anode as both reference (defined as a dynamic hydrogen electrode (DHE)) and counter electrodes was first fed with

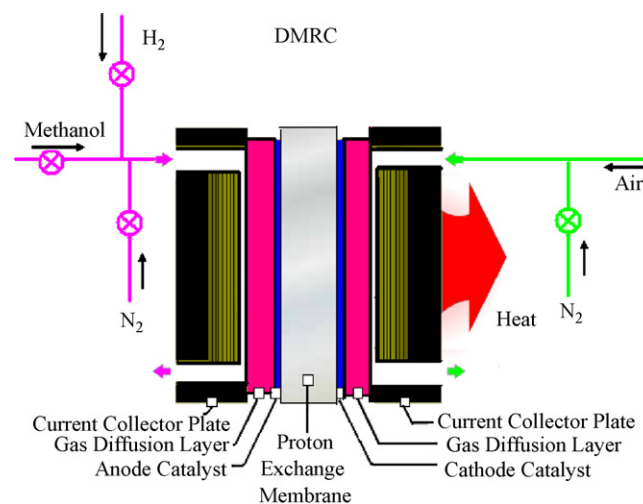


Fig. 1. Scheme of fuel cell set-up including alteration for CV measurements. For CV, air to the cathode was replaced with humidified N₂. The original cathode became the working electrode. For CV methanol solution to the anode was replaced with humidified N₂ for 10 min. N₂ to the anode was replaced with humidified H₂ again and the anode became the counter/reference electrode [23].

Table 1
Maximum power densities (MPD), voltages, and current densities at MPD of the membrane electrode assemblies before and after different test times

MEA no.	MEA 1		MEA 2		MEA 3	
	0 h	117 h	0 h	210 h	0 h	312 h
Current density at MPD (mA cm^{-2}) ^a	200	170	210	180	240	200
Voltage at MPD (V) ^a	0.345	0.307	0.355	0.309	0.34	0.285
MPD (mW cm^{-2}) ^a	69.0	52.2	74.5	55.7	81.5	57.0
Decrement rate (%) ^a	24.3		25.2		30.1	
Current density at 0.4 V (mA cm^{-2})	150	100	170	110	180	110
Decrement (mA cm^{-2})	50		60		70	
Decrement rate (%)	33.3		35.3		38.9	
Power density at 0.4 V (mW cm^{-2})	60.6	40.3	67.9	44.5	71.9	43.7
Decrement (mW cm^{-2})	20.3		23.4		28.2	
Voltage decay rates (mV h^{-1}) ^a	0.40		0.22		0.07	

^a Data were taken from Ref. [23].

nitrogen to purge methanol solution for 10 min, and then nitrogen was replaced with humidified hydrogen gas at a flow rate of 100 mL min^{-1} under ambient pressure. The cathode was first fed with humidified nitrogen to purge air for 10 min, and then stop feeding nitrogen. CV curves were recorded within a potential range of 0.05–1.2 V at a scan rate of 0.02 V s^{-1} . The integrated peak area of hydrogen adsorption–desorption was used to calculate the S_{EAS} of cathodic catalyst. All potential values reported in this work are versus DHE.

2.3. Characterization of physical properties

After electrochemical testing, the MEA was carefully removed from the cell. The cathode GDLs were separated from MEAs after different working times. The membranes with catalyst layers were cut into small pieces for subsequent analysis by XRD and XPS.

2.3.1. X-ray diffraction (XRD)

XRD measurements for the catalyzed GDL were recorded on a Rigaku Ultima III X-ray diffractometer system (Rigaku MSC, Woodlands, TX) using a graphite crystal counter monochromator that filtered Cu K β radiation. The X-ray source was operated at 40 kV and 40 mA. The patterns, recorded in a 2θ range of 20–90°, were obtained using high precision and high resolution parallel beam geometry in a step scanning mode of 1° min^{-1} . The identification of phases was made by referring to the joint committee on powder diffraction standards international center for diffraction data (JCPDS-ICDD) database. Lattice parameters and crystallite sizes were calculated using Jade 7 Plus software (Rigaku). Grain sizes were determined by Scherrer equation using the Pseudo-Voigt profile function.

2.3.2. X-ray photoelectron spectrometry (XPS)

XPS study of surface composition involved a special X-ray photoelectron spectrometer (VG ESCALAB MKII) with the Al K α X-ray source at 1486.6 eV, which recorded the spectra from 45° takeoff-angle at a chamber pressure below 5×10^{-9} Pa. The C 1s electron binding energy was referenced at 284.6 eV, and a non-linear least-squares curve-fitting program was employed with a Gaussian–Lorentzian production function [24,25]. The deconvolution of the XPS spectra was achieved with the reported procedures [26–30].

3. Results and discussion

The changes of PtRu black anodic catalysts with working times were exhibited in our previous works [23]. In this work, we focus

on the change of cathodic catalysts with working times. The performance data of three single DMFCs are also presented in this paper as shown in Table 1 [23]. The discussions on the performance change rules and the performance curves of three individual single cells were presented in detail in reference [23]. A briefly depiction is only provided in here. Compared with the cell performances before the life tests, it can be seen that the maximum power densities (MPD) of DMFCs drop by about 24.3%, 25.2%, and 30.1% after a test time of 117, 210, and 312 h, respectively. The current densities and potentials, at which the MPD occur, also drop with test time. The loss of cell voltage, at which MPD occur, has the greatest value of about 55 mV after the life test of 312 h. The voltage decay rates of DMFCs are about 0.4, 0.22, and 0.07 mV h^{-1} during the tests for 117, 210, and 312 h, respectively. During the overall test, the cell voltages decrease gradually with test time. It can be seen from Table 1 that the current densities of three individual single cells at a cell voltage of 0.4 V after working times of 117, 210, and 312 h decrease by about 50, 60, and 70 mA cm^{-2} , respectively. Power densities at the voltage of 0.4 V decrease by about 20.3, 23.4, and 28.2 mW cm^{-2} after different working times, respectively. Their decrements are 33.3%, 35.3%, and 38.9%, respectively. These indicate that their performance decays are fast at the beginning of working and then are slow down. There is a slow performance loss that is irrecoverable, which may be related to the degradation of catalysts, the dissolution of Nafion® solution in catalyst layers [31], and the aging of polymer electrolyte membrane [12], and so on. With the increasing of working time, the performance loss decreases gradually. The voltage decay rates decrease also evidently with time. Though the decay rate for 312 h is already close to that for the commercialization demands of DMFC [10], it does not meet the demands yet. It is certainly necessary to prolong the life of DMFC.

Fig. 2 shows hydrogen adsorption–desorption curves in cathodes prior to and after the life tests for different working times. The normal peaks of hydrogen adsorption–desorption on pure Pt metal are presented in Fig. 2 before the life tests. The hydrogen adsorption–desorption regions on Pt catalysts decrease gradually with time after the life tests. The two normal peaks of hydrogen desorption also decay gradually with time. The double layer capacitances on three Pt black catalysts are relatively small before the life test. However, their double layer capacitances increase to different extents with time during the life tests. The carbon corrosion happens in gas diffusion layer at higher potentials, higher oxygen content, and higher temperature, which may be the reason for augment of double layer capacitance in cathodes. Furthermore, the small oxidation peaks at about 0.68 V in CV curves before the life tests are attributed to the oxidation of small organic and/or contaminants' molecules adsorbed on Pt metal surface [32]. The peaks

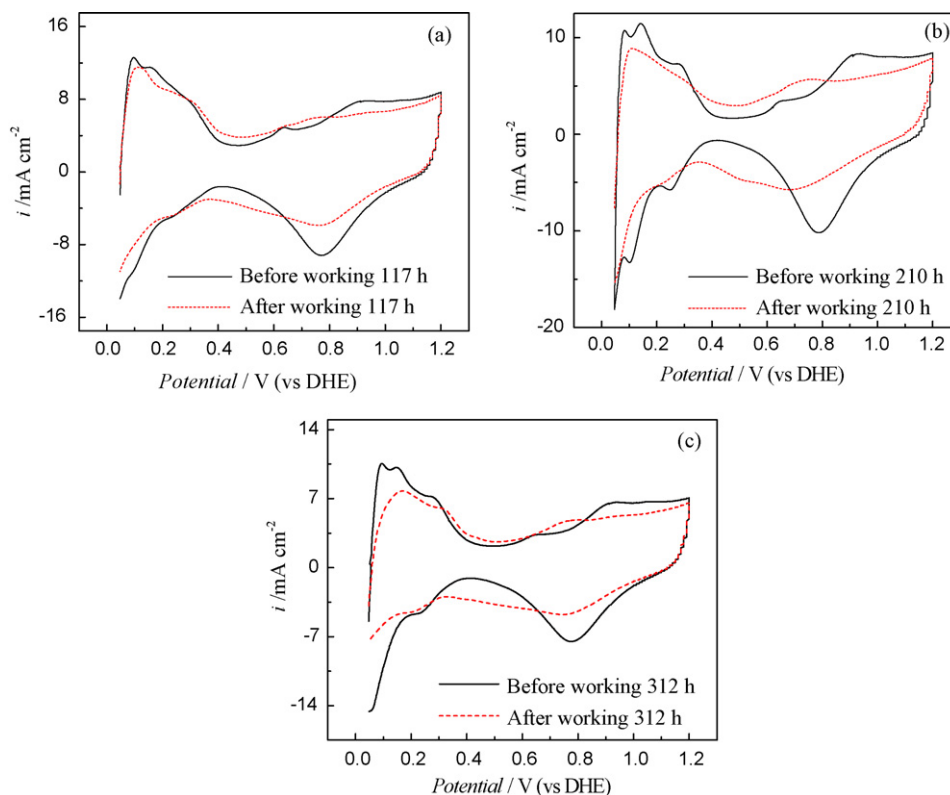


Fig. 2. Hydrogen adsorption–desorption tests of cathodic catalysts before and after different test times. Temperature: 25 °C.

can disappear while more scans are carried out continuously for cathodes.

The electrochemically active surface area (S_{EAS}) is calculated with the recognized method based on hydrogen adsorption–desorption curve [33,34], by Eq. (1) as follows:

$$S_{EAS} = \frac{Q_1}{G \times 210} \quad (1)$$

in which Q_1 is the charge quantity calculated from integrated in CV curves for hydrogen adsorption–desorption in microcoulomb (μC), and a value of 210 ($\mu\text{C cm}^{-2}$) is the charge required to oxidize a monolayer of hydrogen on Pt metal catalyst [35], and G represents the Pt metal loading (mg) in the electrodes.

The results of calculations listed in Table 2 show that the S_{EAS} of cathodic catalysts decrease gradually with time. The S_{EAS} loss after working times of 117, 210, and 312 h are about 24.2%, 35.9%, and

41.3%, respectively. The increments in loss decrease evidently with working time. The changing rates of cathodic catalysts are much higher than those of anodic ones (see Ref. [23]). This result is in agreement with other groups' reports [12,36], indicating that Pt black catalyst and catalyst layer in cathodes already degrade, and the 'triple-phase boundaries' obviously decrease. It means that the performance decay of DMFCs derives from the change of cathodic materials. This is consistent with the result of our previous investigation [17].

After the single cell tests, the used MEA was peeled carefully and cut into small pieces for further analysis. XRD patterns of cathodes were measured as shown in Fig. 3. The diffraction peaks for cathodes at 26 °C can be attributed to the hexagonal graphite structures (002) of the carbon black remaining on the catalyst layer after peeling off from the GDLs. The Pt black has a face-centered cubic (fcc) structure showing the major peaks of (111), (200), (220),

Table 2
Characterization of cathodic catalysts before and after different test times

MEA no.	MEA 1		MEA 2		MEA 3	
	0h	117 h	0h	210 h	0h	312 h
S_{EAS} ($\text{m}^2 \text{g}^{-1}$)	11.19	8.48	10.89	6.98	9.44	5.54
S_{EAS} changing ($\text{m}^2 \text{g}^{-1}$)	2.71		3.91		3.90	
Changing rate (%)	24.2		35.9		41.3	
d_{XRD} (nm)	7.3 ^a	8.3	7.3 ^a	8.7	7.3 ^a	9.2
d_{XRD} changing (nm)	1.0		1.4		1.9	
S_{XRD} ($\text{m}^2 \text{g}^{-1}$)	38.4	33.8	38.4	32.2	38.4	30.5
S_{XRD} changing ($\text{m}^2 \text{g}^{-1}$)	4.6		6.2		7.9	
Changing rate (%)	12.0		16.1		20.4	
Utilization of catalyst (%)	29.1	25.1	28.4	21.7	24.6	18.2
Lattice parameter (Å)	3.9188 ^a	3.9210	3.9188 ^a	3.9197	3.9188 ^a	3.9196

^a Data were taken from Ref. [17].

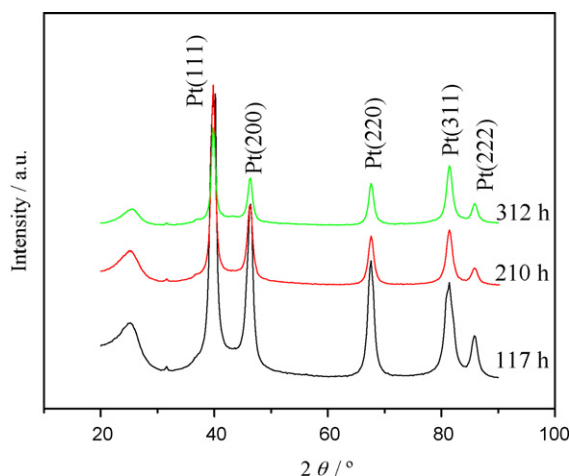


Fig. 3. XRD patterns of cathodic catalysts after different test times.

(311), and so on. The mean particle sizes and lattice parameters of the catalysts before and after the life tests were calculated from XRD patterns by using JADE software. Their results are listed in Table 2. The particle sizes of cathodic catalysts grow from an initial value of 7.3–9.2 nm and their lattice parameters increase from 3.9188 to 3.9210 Å and then decrease to 3.9196 Å with test times. The increments of particle sizes are about 1.0, 1.4, and 1.9 nm after times of 117, 210, and 312 h, respectively. In comparison to those of anode catalysts [23], the sintering rates of cathodic catalysts are evidently higher due to a higher water content and oxygen concen-

tration than in anodes. This result is consistent with Xin's [12,13]. In addition, the higher potential is also adverse to the stability of catalytic particles, especially the unsupported Pt black used in fuel cells [37]. Methanol crossover from anode to cathode must happen during working of DMFC. It is concomitant with performance losses of cathodic catalysts due to the formation of mixed potential on the cathodic catalysts, which is also very deleterious and accelerates the sintering/degradation of cathodic Pt nanoparticles.

The specific surface area of catalysts (denoted as S_{XRD}) calculated from XRD patterns are also listed in Table 2. The loss rate of S_{EAS} in cathode is almost one time higher than that of S_{XRD} as presented in Table 2. It indicates that the agglomeration of catalyst is not the only reason for the S_{EAS} loss in cathode. The Nafion[®] ionomer with catalyst particles desquamates and/or dissolves in the catalyst layer due to their growth, thus results in the decrease of proton conductive paths and 'triple-phase boundaries'. Namely, the S_{EAS} loss increases markedly.

The utilizations (S_{EAS}/S_{XRD}) of catalysts in cathodes decrease with time after the life tests. After a life test of 312 h, the utilization is only 18.2%. However, the utilizations of cathodic catalysts for three MEAs are relatively low, between 25% and 30% before the life tests. So, it is quite necessary to enhance the utilizations of cathodic catalysts. Some work has been done by using different methods to prepare MEAs [38,39]. However, the results are not satisfied yet.

Figs. 4 and 5 represent the curve-fitted Pt 4f, O 1s, and C 1s XPS spectra of Pt black cathodic catalysts prior to and after different working times. The two most intense peaks in Fig. 4a, located at the binding energies of 71.15 eV (Pt 4f_{7/2}) and 74.53 eV (Pt 4f_{5/2}), maintain an area ratio near 4:3 as expected theoretically for pure Pt. Hence they are originated from metallic Pt⁰ without doubt. The peaks at 72.01 and 75.82 eV can be attributed to Pt²⁺ in the form of

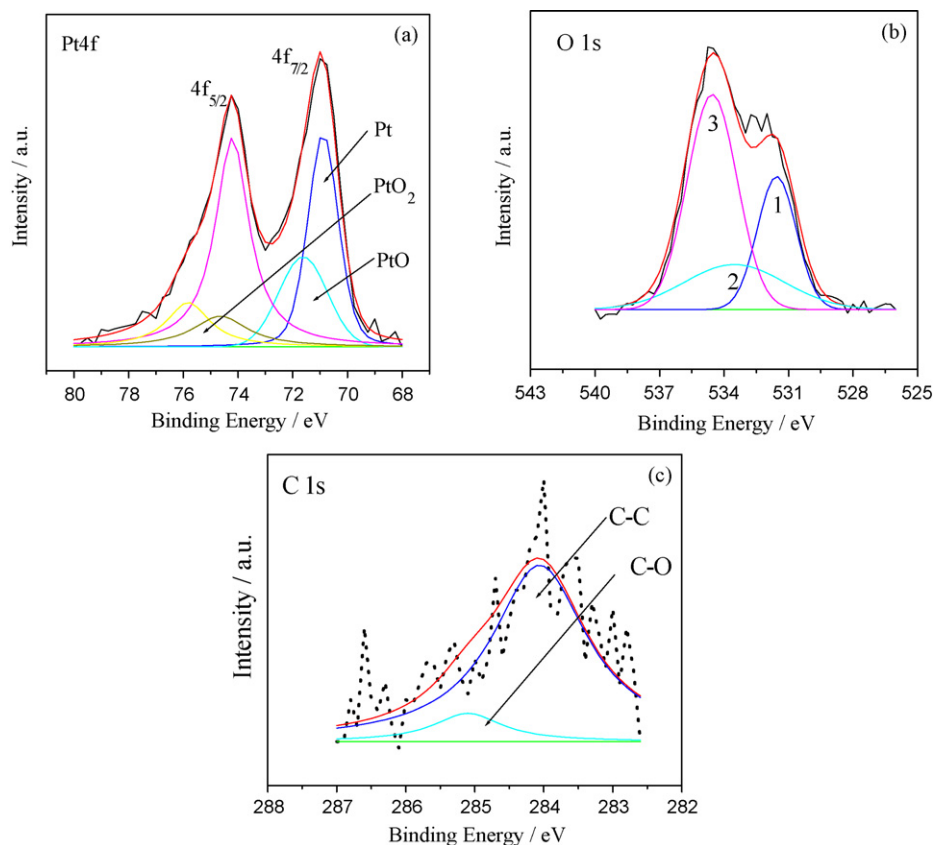


Fig. 4. XPS core level spectra of cathodic catalyst before life test. (a) Pt 4f [17]; (b) O 1s; (c) C 1s.

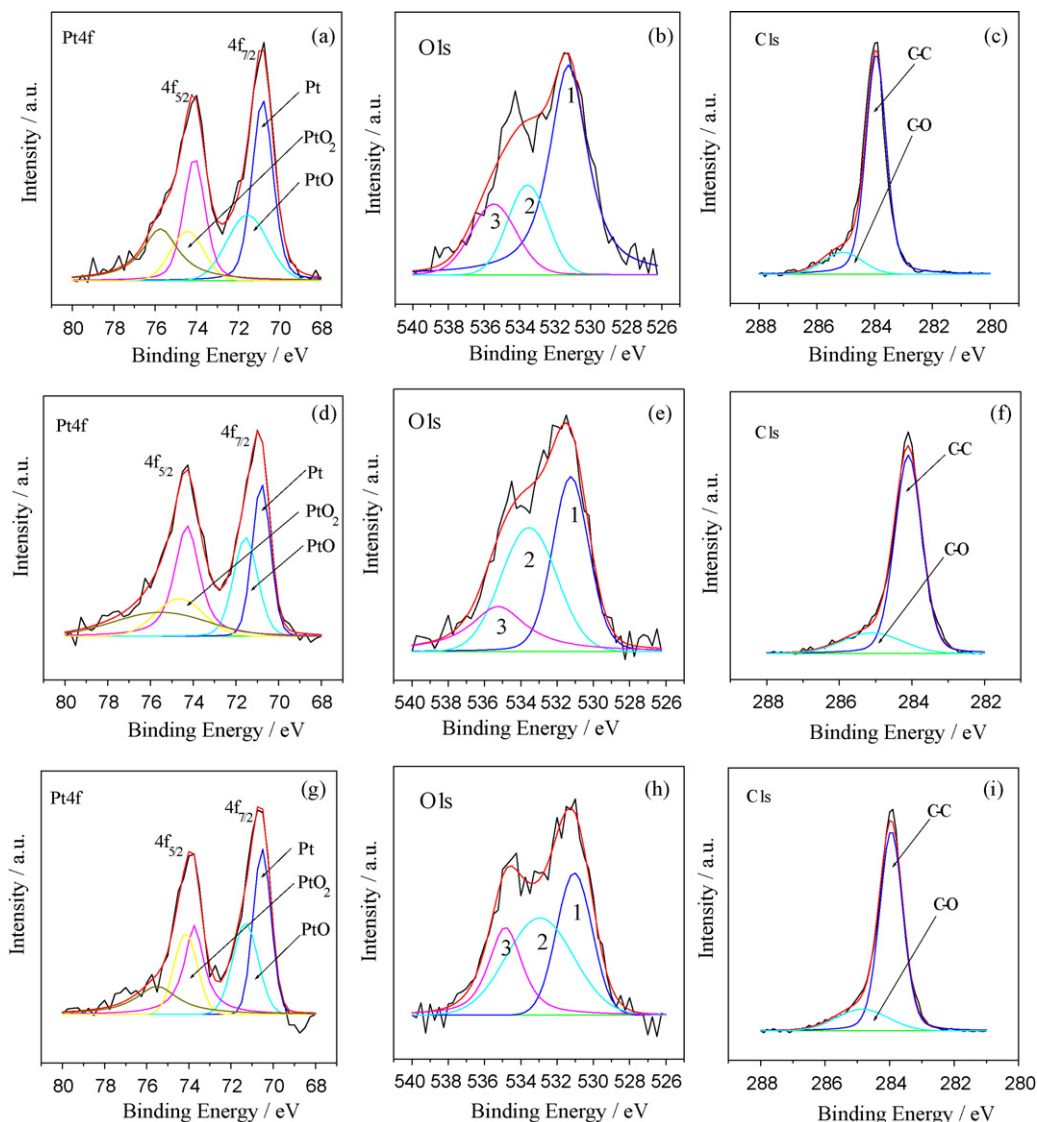


Fig. 5. XPS core level spectra of cathodic catalyst after different test times. (a) Pt 4f after 117 h; (b) O 1s after 117 h; (c) C 1s after 117 h; (d) Pt 4f after 210 h; (e) O 1s after 210 h; (f) C 1s after 210 h; (g) Pt 4f after 312 h; (h) O 1s after 312 h; (i) C 1s after 312 h.

PtO or Pt(OH)₂ [26,28,30], while the peak at 74.65 eV arises from Pt⁴⁺, possibly in PtO₂. The two intense peaks in Fig. 4c, located at the binding energies of 283.95 and 285.10 eV, can be attributed to C–C and C–O bond. The oxidation states of Pt 4f, O 1s, C 1s and their relative amounts are listed in Table 3. The XPS information of C 1s is from GDL.

Table 3

Surface contents of Pt metal, its oxide, and oxygen in cathodic catalysts before and after different test times

Material	Composition	New catalyst	After 117 h	After 210 h	After 312 h
Pt	Pt	64.9 ^a	51.4	49.7	48.3
	PtO	26.0 ^a	38.3	36.6	35.3
	PtO ₂	9.1 ^a	11.4	13.7	16.4
O	1	25.3	60.9	38.8	32.8
	2	22.1	20.1	39.5	42.4
	3	52.6	19.0	21.7	24.8
C	C–C	88.6	85.6	82.7	81.9
	C–O	11.4	14.4	17.3	18.1

^a Data were taken from Ref. [17].

The metal content of Pt black is 64.9%, which is relatively high, and the PtO₂ content is relatively low, only 9.1% in cathode before the life test. The metal contents in cathodes decrease gradually, and the amounts of Pt(II) oxide first increase markedly and then decrease with time after different working times. Their decrements with working time are gradually low. Those are consistent with the performance changes of DMFCs as shown in Table 1. The decrement of Pt metal for 117 h is 20.8%, and for 312 h, it is only 25.6%. However, the amounts of Pt(IV) oxide after life tests increase markedly with time. The increment for 117 h is up to 25.3%, and for 312 h, it is 80.2%. The formation of Pt oxides could have been established as follow:



This is a main reason that results in the increase of Pt(IV) oxide. Methanol crossover is inevitable in DMFC. Methanol from anode can be oxidized to formaldehyde (HCHO) or formic acid (HCOOH) and other intermediates on the Pt catalyst surface in cathode. They are very excellent reducing agents. It is very easy to

deoxidize Pt(IV) oxide. This reducing process can be proposed as follow:



It is reasonable to expect that the Pt nanoparticles during the life test are easily oxidized, dissolved, and then redeposited to grow in a harsh cathodic environment. This is consistent with the proposed mechanism that oxide formation at the cathode is a failure mechanism, i.e. the agglomeration of Pt nanoparticles in cathode is mainly attributed to the dissolution/deposition mechanism. In addition, in accordance with the literature [40–42], O(1s) spectra show an evident presence of –CO species arising from the carbon-support at around 533 eV in all MEAs. The Pt–O or metal-like species are observed in these cathodic catalysts at a binding energy of 531 eV or so. The presence of oxygen containing carbon-functional groups is also seen at a binding energy of about 535 eV in the three MEAs. The contents of –CO species and oxygen containing carbon-functional groups increase gradually with test time. The contents of C–O species in carbon surface increase slowly with working times as presented in Table 3. The results show that the carbon corrosion in GDL already happens by oxygen at higher potentials with higher humidity in cathode than that in anode. In addition, the oxidation process is firstly fast and then slows down with working times. It presents that the corrosion of carbon in contact with Pt should be more rapid. The effect of Pt nanoparticles on carbon corrosion is relatively evident due to the smaller particle size of Pt black at the beginning of the life test. With the increase of working time, the particle size of Pt catalyst grows gradually. The effect of relatively large Pt nanoparticles on carbon corrosion decay slightly as shown in Table 3. It indicates that the carbon corrosion in GDL is the main reason for the increased capacitance of double layer in cyclic voltammograms as shown in Fig. 2.

Cathodic catalyst in DMFC operates in a harsh environment of high water content, low pH value, high temperature, high potentials, and high oxygen partial pressures coupled with the poisoning of methanol crossover from anode and the formation of the mixed potential on the cathodic catalyst surface. Which one is the main factor? This is an open question. A lot of work needs to do to explore the effect degree of each factor on the degradation of cathodic catalyst.

4. Conclusions

The particle sizes of Pt black catalysts in DMFC increase gradually with time. The cathode potential is relatively high and has a strong adverse influence on cathodic catalyst in comparison to the anode one. The contents of Pt metal in cathodes decrease, but the contents of Pt(IV) oxide increase markedly with test time. The electrochemically active surface areas (S_{EAS}) of cathodic catalysts decrease markedly with test time. The loss rate of S_{EAS} of the cathode is much higher than that of S_{XRD} . The utilizations of catalysts also lower evidently. The decrease of both S_{EAS} and utilizations of cathodic catalysts and the dissolution of Pt metal from cathodic catalysts surface are the main factors affecting the performance decay of DMFCs. It accords with the dissolution/deposition mechanism for the aging of cathodic catalysts.

Acknowledgements

This work is supported financially by the National Natural Science Foundation of China (Grant No. 20606007), the Scientific

Research Foundation for the Returned Overseas Chinese Scholars, State Education Ministry (2008), Postdoctoral Science–Research Developmental Foundation of Heilongjiang Province of China (LBH-Q07044), and Harbin Innovation Science Foundation for Youths (2007RFQXG042).

References

- [1] M.K. Debe, A.K. Schmoeckel, G.D. Vernstrom, R. Atanasoski, J. Power Sources 161 (2006) 1002–1011.
- [2] E. Antolini, J.R.C. Salgado, E.R. Gonzalez, J. Power Sources 160 (2006) 957–968.
- [3] Z.B. Wang, G.P. Yin, P.F. Shi, Carbon 44 (2006) 133–140.
- [4] T.R. Ralph, M.P. Hogarth, Platinum Met. Rev. 46 (2002) 3–14.
- [5] H.R. Colón-Mercado, B.N. Popov, J. Power Sources 155 (2006) 253–263.
- [6] S.C. Thomas, X.M. Ren, S. Gottesfeld, P. Zelenay, Electrochim. Acta 47 (2002) 3741–3748.
- [7] V. Gogel, T. Frey, Y.S. Zhu, K.A. Friedrich, L. Jörissen, J. Garche, J. Power Sources 127 (2004) 172–180.
- [8] Z.B. Wang, G.P. Yin, J. Zhang, Y.C. Sun, P.F. Shi, Electrochim. Acta 51 (2006) 5691–5697.
- [9] Y.Y. Shao, G.P. Yin, Y.Z. Gao, J. Power Sources 171 (2007) 558–566.
- [10] S.D. Knights, K.M. Colbow, J. St-Pierre, D.P. Wilkinson, J. Power Sources 127 (2004) 127–134.
- [11] S.-Y. Ahn, S.-J. Shin, H.Y. Ha, S.-A. Hong, Y.-C. Lee, T.W. Lim, I.-H. Oh, J. Power Sources 106 (2002) 295–303.
- [12] W.M. Chen, G.Q. Sun, J.S. Guo, X.S. Zhao, S.Y. Yan, J. Tian, S.H. Tang, Z.H. Zhou, Q. Xin, Electrochim. Acta 51 (2006) 2391–2399.
- [13] L.H. Jiang, G.Q. Sun, S.L. Wang, G.X. Wang, Q. Xin, Z.H. Zhou, B. Zhou, Electrochim. Commun. 7 (2005) 663–668.
- [14] M.S. Wilson, F.H. Garzon, K.E. Sickafus, S. Gottesfeld, J. Electrochem. Soc. 140 (1993) 2872–2877.
- [15] Y.Y. Shao, G.P. Yin, Y.Z. Gao, P.F. Shi, J. Electrochem. Soc. 153 (2006) A1093–A1097.
- [16] J.G. Liu, Z.H. Zhou, X.X. Zhao, Q. Xin, G.Q. Sun, B.L. Yi, Phys. Chem. Chem. Phys. 6 (2004) 134–137.
- [17] Z.B. Wang, H. Rivera, X.P. Wang, H.X. Zhang, X.P. Feng, E.A. Lewis, E.S. Smotkin, J. Power Sources 177 (2008) 386–392.
- [18] P. Ascarelli, V. Contini, R. Giorgi, J. Appl. Phys. 91 (2002) 4556–4561.
- [19] J.A. Bett, K. Kinoshita, P. Stonehart, J. Catal. 35 (1974) 307–316.
- [20] J.A.S. Bett, K. Kinoshita, P.J. Stonehart, J. Catal. 41 (1976) 124–133.
- [21] P.J. Ferreira, G.J. la O', Y. Shao-Horn, D. Morgan, R. Makharia, S. Kocha, H.A. Gasteiger, J. Electrochem. Soc. 152 (2005) A2256–A2271.
- [22] C.G. Granqvist, R.A. Buhrman, J. Catal. 42 (1976) 477–479.
- [23] Z.B. Wang, X.P. Wang, P.J. Zuo, B.Q. Yang, G.P. Yin, X.-P. Feng, J. Power Sources 181 (2008) 93–100.
- [24] K.W. Park, J.H. Choi, B.K. Kwon, S.A. Lee, Y.E. Sung, H.Y. Ha, S.A. Hong, H.S. Kim, A. Wieckowski, J. Phys. Chem. B 106 (2002) 1869–1877.
- [25] C. Bock, C. Paquet, M. Couillard, G.A. Botton, B.R. MacDougall, J. Am. Chem. Soc. 126 (2004) 8028–8037.
- [26] F.J. Rodriguez-Nieto, T. Morante-Catacora, C.R. Cabrera, J. Electroanal. Chem. 571 (2004) 15–26.
- [27] A.S. Arico, G. Monforte, E. Modica, P.L. Antonucci, V. Antonucci, Electrochim. Commun. 2 (2000) 466–470.
- [28] A.K. Shukla, A.S. Arico, K.M. El-Khatib, H. Kim, P.L. Antonucci, V. Antonucci, Appl. Surf. Sci. 137 (1999) 20–29.
- [29] Y.M. Liang, H.M. Zhang, Z.Q. Tian, X.B. Zhu, X.L. Wang, B.L. Yi, J. Phys. Chem. B 110 (2006) 7828–7834.
- [30] Z.B. Wang, G.P. Yin, Y.G. Lin, J. Power Sources 170 (2007) 242–250.
- [31] L.C. DeBolt, U.W. Suter, Macromolecules 20 (1987) 1425–1428.
- [32] J.M. Rheaume, B. Muller, M. Schulze, J. Power Sources 76 (1998) 60–68.
- [33] A. Pozio, M. De Francesco, A. Cenni, F. Cardellini, L. Giorgi, J. Power Sources 105 (2002) 13–19.
- [34] C.L. Green, A. Kucernak, J. Phys. Chem. B 106 (2002) 1036–1047.
- [35] J.H. Jiang, A. Kucernak, Chem. Mater. 16 (2004) 1362–1367.
- [36] S.C. Thomas, X. Ren, S. Gottesfeld, J. Electrochem. Soc. 146 (1999) 4354–4359.
- [37] K.H. Choi, H.S. Kim, T.H. Lee, J. Power Sources 75 (1998) 230–235.
- [38] H.L. Tang, S.L. Wang, S.P. Jiang, M. Pan, J. Power Sources 170 (2007) 140–144.
- [39] C.H. Hsu, C.C. Wan, J. Power Sources 115 (2003) 268–273.
- [40] A.K. Shukla, M. Neergat, P. Bera, V. Jayaram, M.S. Hegde, J. Electroanal. Chem. 504 (2001) 111–119.
- [41] A.S. Arico, A.K. Shukla, H. Kim, S. Park, M. Min, V. Antonucci, Appl. Surf. Sci. 172 (2001) 33–40.
- [42] A.S. Arico, P. Creti, P.L. Antonucci, J. Cho, H. Kim, V. Antonucci, Electrochim. Acta 43 (1998) 3719–3729.